Aspects of Molecular Medicine 2 (2023) 100021

Contents lists available at ScienceDirect

Aspects of Molecular Medicine

journal homepage: www.journals.elsevier.com/aspects-of-molecular-medicine

Curcumin and butyrate induce fibroblast senescence without the emergence of fibrosis biomarkers

Siwei Chu [a], Natali Joma [b,c], Hui Wen Yong [c], Dusica Maysinger [b], Ashok Kakkar [c,**], Ursula Stochaj [a,d,*]

[a] Department of Physiology, McGill University, Montreal, Canada
[b] Department of Pharmacology and Therapeutics, McGill University, Montreal, Canada
[c] Department of Chemistry, McGill University, Montreal, Canada
[d] Quantitative Life Sciences Program, McGill University, Montreal, Canada

ARTICLE INFO

Handling Editor: Prof A Angelo Azzi

Keywords:
Curcumin
Curcumin nanoformulation
Butyrate
Fibroblasts
Cellular senescence

ABSTRACT

Background: Small molecules have emerged as valuable tools to modulate cellular homeostasis and the changes associated with aging. In particular, the phytochemical curcumin elicits cytoprotective effects that promote human health and longevity. The short-chain fatty acid butyrate provides anti-fibrotic activities, but can also induce cellular senescence.

Rationale: The impact of curcumin and butyrate on living cells are not fully understood. To obtain this information, our work focuses on fibroblasts. We selected fibroblasts as cellular model, because they (i) are present in different tissues and organs, (ii) contribute essential functions that derail during organismal aging, and (iii) are prime targets for therapeutic interventions that ameliorate aging-related pathologies.

Methods and results: A panel of quantitative assessments determines how curcumin and its nanoformulation (nano-curcumin), either alone or in combination with butyrate, modulate fibroblast physiology. Several experimental approaches and biomarkers demonstrate that curcumin (i) diminishes fibroblast viability, and (ii) promotes cellular senescence in a concentration-dependent fashion. Specifically, curcumin and nano-curcumin increase the activity of senescence-associated β-galactosidase and reduce the abundance of lamin B. When combined with butyrate, both curcumin and nano-curcumin enhance cell death and senescence. Free curcumin decreases the levels of Nrf2, a transcription factor that is upregulated upon oxidative stress. Neither curcumin nor nano-curcumin changes the abundance of the transcription factor NFκB, which is critical for inflammatory responses. Free curcumin, butyrate and nano-curcumin/butyrate combinations significantly diminish the abundance of the lysine deacetylase SIRT1, which is a key regulator of cellular senescence. Notably, none of the compounds or their combinations elevates biomarkers of fibrosis.

Conclusions: This study defines the cellular and molecular changes produced in fibroblasts by curcumin, nano-curcumin, alone or together with butyrate. Collectively, our results set the stage to explore curcumin/butyrate-based treatments to control the cellular activities that are contributed by fibroblasts.

1. Introduction

Cellular senescence is a critical regulator of organismal aging, development, tissue regeneration, and cell plasticity (Ring et al., 2022; Tripathi et al., 2021). Organismal homeostasis declines during aging; fibroblasts are particularly important for these aging-related changes (Plikus et al., 2021). Present in many organs and tissues, fibroblasts respond to tissue damage and other cues (Kirk et al., 2021). For instance, wound healing requires a subpopulation of fibroblasts to undergo senescence (Tripathi et al., 2021). Damage-induced fibroblast activation generates contractile myofibroblasts that advance tissue repair (Plikus et al., 2021). However, the persistence of myofibroblasts can also promote fibrosis in multiple tissues and organs (McElhinney et al., 2023; Plikus et al., 2021).

Exploration of the molecular mechanisms that drive cellular senescence inspired the development of pharmacological tools to eliminate senescent cells (Lagoumtzi and Chondrogianni, 2021; Robbins et al.,

* Corresponding author. Department of Physiology, McGill University, Montreal, Canada.
** Corresponding author.
E-mail addresses: ashok.kakkar@mcgill.ca (A. Kakkar), ursula.stochaj@mcgill.ca (U. Stochaj).

https://doi.org/10.1016/j.amolm.2023.100021
Received 18 July 2023; Received in revised form 7 August 2023; Accepted 11 August 2023
Available online 12 August 2023

Abbreviations

ECL	enhanced chemiluminescence
DMSO	dimethyl sulfoxide
DL	drug loading
DLS	dynamic light scattering
EE	encapsulation efficiency
NaBu	sodium butyrate
Nano-curcumin	curcumin nanoformulation
NP	nanoparticle
SA-β-gal	senescence-associated β-galactosidase
TBST	Tris-buffered saline containing 0.05% Tween 20
TEM	transmission electron microscopy
X-gal	5-bromo-4-chloro-3-indolyl β-D-galactopyranoside

2020). Various phytochemicals, such as curcumin, function as senolytics or senomorphics, at least in some cell types (Lagoumtzi and Chondrogianni, 2021). Several of these senotherapeutics are currently evaluated in clinical trials (Chaib et al., 2022; NIH, Clinical Trials, 2023).

Curcumin is a natural product with numerous health benefits, including anti-oxidant and anti-inflammatory activities (Mahjoob and Stochaj, 2021). This cytoprotective polyphenol prevents or reduces aging-related dysfunctions in experimental model systems. Accordingly, curcumin is a promising compound for clinical applications (Mahjoob and Stochaj, 2021; NIH, Clinical Trials, 2023).

Due to its poor solubility in aqueous solutions and metabolic turnover in living organisms, curcumin has low bioavailability (Ataei et al., 2023). One of the major strategies to enhance curcumin's bioavailability is the generation of curcumin-loaded nanomaterials (Ataei et al., 2023; Mahjoob and Stochaj, 2021). In particular, curcumin nanoformulations have evolved as promising alternatives to administrating the free compound. Tunable nanocarriers that are non-toxic to normal cells are ideal candidates for the delivery of curcumin (Moquin et al., 2019).

Like curcumin, the short-chain fatty acid butyrate improves human health. As cellular homeostasis declines during aging, tissues and organs become more prone to fibrosis (Han et al., 2023; Li et al., 2022; Yi et al., 2023). Accordingly, the antifibrotic actions of butyrate are directly relevant to aging (Corrêa et al., 2022; Park et al., 2021).

Curcumin may function as a senolytic that eliminates senescent cells *in vitro* (Li et al., 2019). At present, it is not fully understood which cell types are responsive to the senolytic activity of curcumin. It is also not known whether curcumin prevents the onset of senescence in cells of diverse origin, such as fibroblasts. Building on our previous experience with senescent cells (Chu et al., 2022), we addressed these questions in NIH3T3 cells. This fibroblast cell line was established from 17 to 19 days old mouse embryos (Todaro and Green, 1963) and has been explored for aging research (for example (Chang et al., 2019; Chu et al., 2022)). Our study reveals that curcumin triggers fibroblast senescence and enhances the senescent phenotype produced by butyrate. Moreover, curcumin, either alone or in combination with butyrate, regulates tissue homeostasis through the induction of fibroblast senescence, but without promoting fibrosis.

2. Materials and methods

2.1. Primary and secondary antibodies

Primary antibodies and their dilutions for Western blotting are listed in Table 1. Affinity-purified HRP-conjugated secondary antibodies were obtained from Jackson ImmunoResearch and used at a 1:2,000 dilution.

Table 1
Primary antibodies for Western blotting.

Antigen	Source of Antibody	Dilution for Western blotting
p21	Santa Cruz Biotechnology, sc-397	1:500
p53	Cell Signaling Technology; #2524	1:1,000
Lamin B	Santa Cruz Biotechnology, sc-6216	1:1,000
γH2AX	Sigma-Aldrich, clone JBW301, 05-636	1:2,000
Nrf2	Santa Cruz Biotechnology, sc-722	1:500
NFκB	Santa Cruz Biotechnology, sc-372	1:1,000
SIRT1	ABclonal, A0230	1:1,000
α-Smooth muscle actin (SMA)	ABclonal, A1011	1:2,000
Myosin light chain (MLC)	Sigma-Aldrich, M4401	1:2,000
Actin	Chemicon MAB1501	1:100,000

2.2. Synthesis of miktoarm polymer

AB_2 (A = polycaprolactone, PCL; B = polyethylene glycol, PEG) miktoarm polymer (M1) was synthesized by adaptation of the procedure reported earlier (Baghbanbashi et al., 2022; Lotocki et al., 2021; Soliman et al., 2010; Yong and Kakkar, 2021). Briefly, 3,5-dihydroxybenzylalcohol was dipropargylated, and the resulting compound was used as an initiator for ring-opening polymerization of ε-caprolactone to obtain $(alkyne)_2$-core-PCL. Methoxy-PEG_{2000}-N_3 was separately prepared from commercially available methoxy-PEG_{2000}-OH, by reacting it first with tosyl chloride and then sodium azide. Methoxy-PEG_{2000}-N_3 was then reacted with $(alkyne)_2$-core-PCL using copper catalyzed alkyne-azide cycloaddition (click) chemistry. The resulting branched polymer (M1, Fig. 1) was characterized using ^1H (Fig. S1), ^{13}C NMR (Fig. S2) and GPC, and the data agreed well with our previously published work (Baghbanbashi et al., 2022; Lotocki et al., 2021). The molecular mass of M1 was determined as 7,900 g/mol.

2.3. Aqueous self-assembly

Curcumin loaded nanoformulations from the miktoarm polymer were prepared using the cosolvent evaporation method (Baghbanbashi et al., 2022; Lotocki et al., 2021; Soliman et al., 2010; Yong and Kakkar, 2021). Briefly, 5 mg of M1 was dissolved in 2 mL of HPLC-grade acetone, and 1 mg/mL of curcumin in HPLC grade acetone solution was prepared separately. 0.5 mL of this curcumin solution was added to the above M1 solution and sonicated for 5 min before adding the mixture slowly dropwise into 2 mL of Milli-Q H_2O while stirring. The acetone was then allowed to evaporate overnight in the dark. Subsequently, the solution was centrifuged at 1000 rpm for 10 min and the supernatant was passed through a 0.22 μm PVDF syringe filter. Blank formulations were prepared by following a similar procedure without mixing curcumin solution with M1 solution in 2 mL of acetone.

2.4. Determination of loading capacity and encapsulation efficiency

To calculate the drug loading (DL) and encapsulation efficiency (EE), 20 μL of the micelle solution was collected and diluted to 2 mL with methanol. The solution was then analyzed with UV–Vis. The amount of curcumin present was calculated using the absorption intensity of the diluted solution at 426 nm and the gradient of the standard calibration curve of curcumin in methanol. The DL and EE were then calculated using following equations:

DL%= [Loaded drug/ (Total drug + polymer added)] *100%

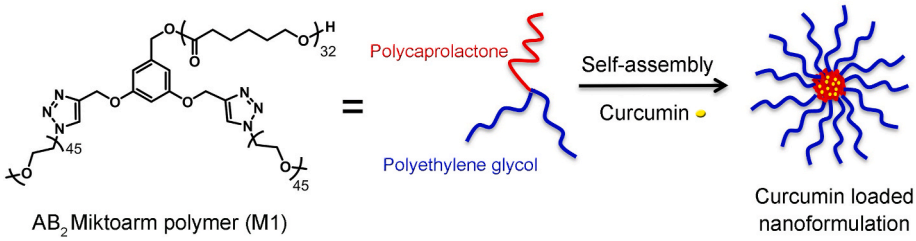

Fig. 1. Structure of miktoarm polymer M1 and its aqueous self-assembly, leading to core-shell curcumin (yellow) loaded nanoformulations. The polycaprolactone is depicted in red, and polyethylene glycol arms are shown in blue. (For interpretation of the references to colour in this figure legend, the reader is referred to the Web version of this article.)

EE%= [Loaded drug/ Total drug added] *100%

2.5. Characterization of nanoparticles

Aqueous self-assemblies from miktoarm polymer M1 were analyzed using dynamic light scattering (DLS) and transmission electron microscopy (TEM). DLS provides a measure of the hydrodynamic diameter of the nanoparticles, while TEM visualizes the nanoparticle morphology and size without hydration sphere. The spherical core-shell micelles had a hydrodynamic diameter of 60 ± 6 nm (blank), which increased to 65 ± 8 nm upon loading with curcumin. Using TEM, spherical micelles had an average size of 40 nm (blank) and 50 nm (nano-curcumin), respectively (Table 2). In addition to different output (hydrodynamic diameter with DLS), the smaller sizes of nanoparticles determined with TEM (in comparison to DLS) are attributed to the shrinking of micelles upon dehydration during sample preparation. The encapsulation of curcumin into M1-based micelles led to loading capacity of 7.7 ± 0.6% and encapsulation efficiency of 84.8 ± 7.1%. It resulted in approximately 700x increase in curcumin solubility.

2.6. Growth and treatment of NIH3T3 cells

NIH3T3 fibroblasts were grown in Dulbecco's modified eagle medium (DMEM), supplemented with 8% bovine calf serum (BCS) and 1% penicillin/streptomycin (Chu et al., 2022). Cultures were kept at 37 °C in a humidified atmosphere containing 5% CO_2. Senescence induction with sodium butyrate (here referred to as butyrate) has been described earlier (Chu et al., 2022). In brief, sodium butyrate (Alfa Aesar) was dissolved in sterile distilled water. The concentration of the sodium butyrate stock solution was 100 mM. To induce cellular senescence, NIH3T3 fibroblasts were incubated with growth medium containing 5 mM sodium butyrate. Vehicle controls for butyrate were cultured in growth medium supplemented with sterile distilled water.

Treatment with curcumin or nano-curcumin. Curcumin (Sigma, C1386) was dissolved in dimethyl sulfoxide (DMSO; Fisher BioReagents). For vehicle controls and curcumin treatments, the final DMSO concentration was 0.2% (v/v). Curcumin stock solutions (500 ×) were diluted in pre-warmed medium immediately before addition to the cells. Curcumin-loaded nanoparticles (nano-curcumin) were suspended in distilled water. Nano-curcumin was added to achieve the same final concentrations of curcumin as for the free compound. Two types of control groups were included for nano-curcumin, (i) sterile water to monitor the effects of the nanocarrier, (ii) nanoparticles only (without curcumin loading). Sterile water is represented in Figs. 4 and 5 as "− NPs, 0 μM Cur". Empty nanoparticles are indicated by "+ NPs, 0 μM Cur".

Nanoparticles were present at concentrations that are above the critical micelle concentration (CMC). The CMC for the nanoparticles used in our study is 3.43 μg/ml.

Curcumin or nano-curcumin treatment followed by sodium butyrate incubation. Fibroblasts were cultured in medium containing free curcumin or nano-curcumin for two days. Cells were then cultured for additional three days in medium containing free curcumin or nano-curcumin and sodium butyrate or the vehicle water.

Table 2
Properties of nanocarriers.

	D_H (nm)[a]	D_{TEM} (nm)[b]	Loading capacity (%)	Encapsulation efficiency (%)
M1 based blank micelles	60 ± 6	40	not applicable	not applicable
Curcumin-loaded M1 based micelles	65 ± 8	50	7.7 ± 0.6	84.8 ± 7.1

[a] Hydrodynamic, diameter determined by dynamic light scattering.
[b] Diameter, measured by transmission electron microscopy.

2.7. Cell viability assay

Cell viability was measured with a resazurin (Acros Organics) reduction assay (Uzarski et al., 2017). This assay uses resazurin, a non-fluorescent and cell-permeable dye. Viable cells reduce resazurin to generate the fluorescent product resorufin. The number of viable cells is proportional to the amount of resorufin generated (Riss TL et al., 2013 [updated 2016]). To monitor cell viability, fibroblasts were seeded in 96-well plates and treated as described in section 2.6. Non-specific background signals were determined with wells that received growth medium and the assay solutions, but no cells. Following treatment, 20 μl of resazurin solution (150 μg/ml in PBS, filtered before use) was added to each well. Samples were incubated at 37 °C and resorufin fluorescence (excitation/emission: 560 nm/590 nm) was measured with a plate reader (Tecan Infinite M1000).

2.8. Evaluation of senescence-associated β-galactosidase

The enzymatic activity of senescence-associated beta-galactosidase (SA-β-gal) correlates with cellular senescence and is commonly used as a marker to identify senescent cells. SA-β-gal activity can be visualized at pH 6.0 with 5-bromo-4-chloro-3-indolyl β-D-galactopyranoside (X-gal) as the chromogenic substrate (Debacq-Chainiaux et al., 2009). For the study described here, fibroblasts were seeded on coverslips in 24-well plates and treated as described in section 2.6. Following treatment, cells were washed twice with PBS, fixed for 5 min in PBS containing 2% formaldehyde and 0.2% glutaraldehyde, and washed twice with PBS. Samples were then incubated with staining solution (40 mM citric acid/Na buffer, 5 mM $K_4[Fe(CN_6)]\cdot 3H_2O$, 5 mM $K_3[Fe(CN_6)]$, 150 mM NaCl, 2 mM $MgCl_2$, 1 mg/ml X-gal, dissolved in distilled water) overnight at 37 °C (500 μl per well). The staining solution was removed on the next day; coverslips were washed twice with PBS, and mounted on a microscope slide. Coverslips were sealed with nail polish, and imaged with a Leica Galen III microscope using a 20 × objective (Chu et al., 2022). At least 100 cells per condition were evaluated for each

independent experiment.

2.9. Western blotting

The preparation of crude cell extracts and Western blotting protocols were described earlier (Chu et al., 2022; Moujaber et al., 2019). In brief, cells were grown on 10 cm culture dishes and incubated with the appropriate vehicle, curcumin, or nano-curcumin, and butyrate. Following treatment, cells were washed twice with PBS, and stored at −70 °C until use. Crude extracts were prepared as published (Chu et al., 2022; Moujaber et al., 2019). Samples were separated on polyacrylamide gels and transferred to nitrocellulose filters. Filters were blocked in Tris-buffered saline containing 0.05% Tween 20 (TBST) and 5% nonfat milk for 1 h at room temperature. After incubation with primary antibodies (4 °C, overnight), filters were washed in TBST (1 h, room temperature), and incubated with HRP-conjugated secondary antibodies (4 °C, overnight). After washing, signals were detected for enhanced chemiluminescence (ECL, BioRad, Clarity Western ECL substrate). ECL-signals were captured with a ChemiDoc™ imager. Details on the primary antibodies used for Western blotting are shown in Table 1. Images of the original blots are included in the Supplemental file.

2.10. Statistical evaluation

Statistical evaluation was performed with One-way ANOVA and Bonferroni correction. Each dataset represents between two and three independent experiments. The number of independent experiments is stated in the figure legends. Pairwise comparisons to controls were conducted. The effect of curcumin was assessed separately for experimental groups treated (i) without or (ii) with sodium butyrate. Student's t-test was used to assess two experimental groups.

3. Results and discussion

3.1. Curcumin and nano-curcumin diminish fibroblast viability in a concentration-dependent fashion

A first set of experiments identified curcumin concentrations with low toxicity for NIH3T3 cells. While 0.1 μM and 1 μM curcumin had no marked effect, the viability significantly declined for 10 μM curcumin after 3 or 5 days of incubation (Fig. 2a). Based on these results, we selected 1 μM and 10 μM curcumin for all subsequent work. These curcumin concentrations can be achieved *in vivo* (Bielak-Zmijewska et al., 2019; El-Saadony et al., 2022). For example, 1 h after oral administration of 4–8 g of curcumin, plasma concentrations varied between 0.4 and 3.6 μM to human subjects (Cheng et al., 2001). Curcumin serum concentrations can be markedly increased when the compound is administered with adjuvants or as nanoformulation (Dei Cas and Ghidoni, 2019; Heidari et al., 2023; Mahjoob and Stochaj, 2021). Butyrate, used for some of our experiments, is naturally produced by the gut microbiome; it reaches millimolar concentrations *in vivo* (Chriett et al., 2019).

Developed from a miktoarm polymer, a non-toxic carrier was evaluated in parallel for curcumin delivery. Soft nanoparticles from amphiphilic block-copolymers overcome the obstacles of curcumin low bioavailability and short half-life in biological environments (Li et al., 2020). We have used branched star polymers of AB_2 composition (A = polycaprolactone, hydrophobic biocompatible and biodegradable arm; B = polyethylene glycol, hydrophilic arms that confer aqueous solubility and stealth to the nanoformulation), to develop nano-curcumin for this study (see Materials and methods for details). AB_2 amphiphilic star block copolymers self-assemble into a core–shell micelle structure in an aqueous medium, yielding nanoparticles with smaller hydrodynamic diameters, much denser core-corona structure, lower critical micelle concentrations, and higher lipophilic cargo efficiencies compared to their linear analogs (Kakkar et al., 2017; Lotocki and Kakkar, 2020). For our experiments, these nanoparticles were loaded with curcumin. The curcumin nanoformulation, referred to as nano-curcumin, was assessed in parallel. As observed with free curcumin, high concentrations of nano-curcumin also diminished the viability of fibroblasts (Fig. 2b). However, the effect was less prominent when compared with the free compound.

3.2. Curcumin and nano-curcumin promote senescence and enhance butyrate-induced senescence in fibroblasts

The evaluation of senescence-associated β-galactosidase (SA-β-gal) revealed that free and nano-curcumin triggered fibroblast senescence (Fig. 3). Notably, curcumin and nano-curcumin did not block the onset of butyrate-induced senescence. Compared to the individual agents, curcumin/butyrate or nano-curcumin/butyrate combinations further increased the percentage of senescent cells (Fig. 3). These combinations also markedly reduced fibroblast viability (Fig. 3). At 10 μM, free curcumin caused significantly more cellular senescence when compared with nano-curcumin. At the same time, cell viability was significantly

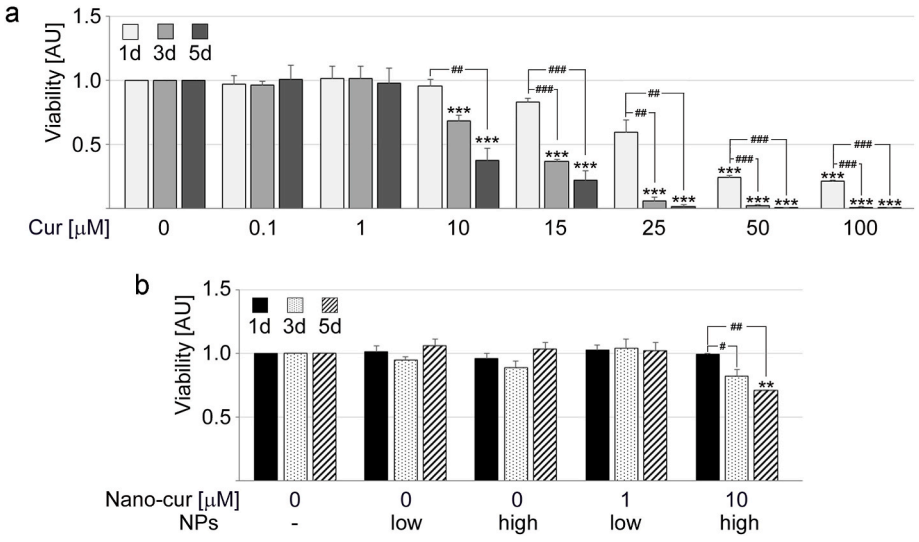

Fig. 2. Effect of free and nano-curcumin on fibroblast viability. NIH3T3 cell viability was measured after treatment with different forms of curcumin. The graphs represent averages of three independent experiments (n = 3). (a) Cells were treated for 1, 3, or 5 days with the free curcumin concentration indicated. (b) Fibroblasts were incubated with vehicle, empty nanoparticles, or nanoparticles loaded with curcumin (Nano-cur). Concentrations of empty nanoparticles (low, high) were matched to the nanocarriers provided as nano-curcumin. Treatment was for 1, 3, or 5 days with final curcumin concentrations of 1 μM or 10 μM. (a, b) One-way ANOVA combined with Bonferroni correction uncovered significant differences between controls (no curcumin or no curcumin, no nanoparticles) and treated samples (**, $p < 0.01$; ***, $p < 0.001$). One-way ANOVA and Bonferroni posthoc analysis also assessed the effects of incubation time for a specific curcumin or nano-curcumin concentration. Pairwise comparisons were made relative to day 1 (#, $p < 0.05$; ##, $p < 0.01$; ###, $p < 0.001$). AU, arbitrary units; NPs, nanoparticles.

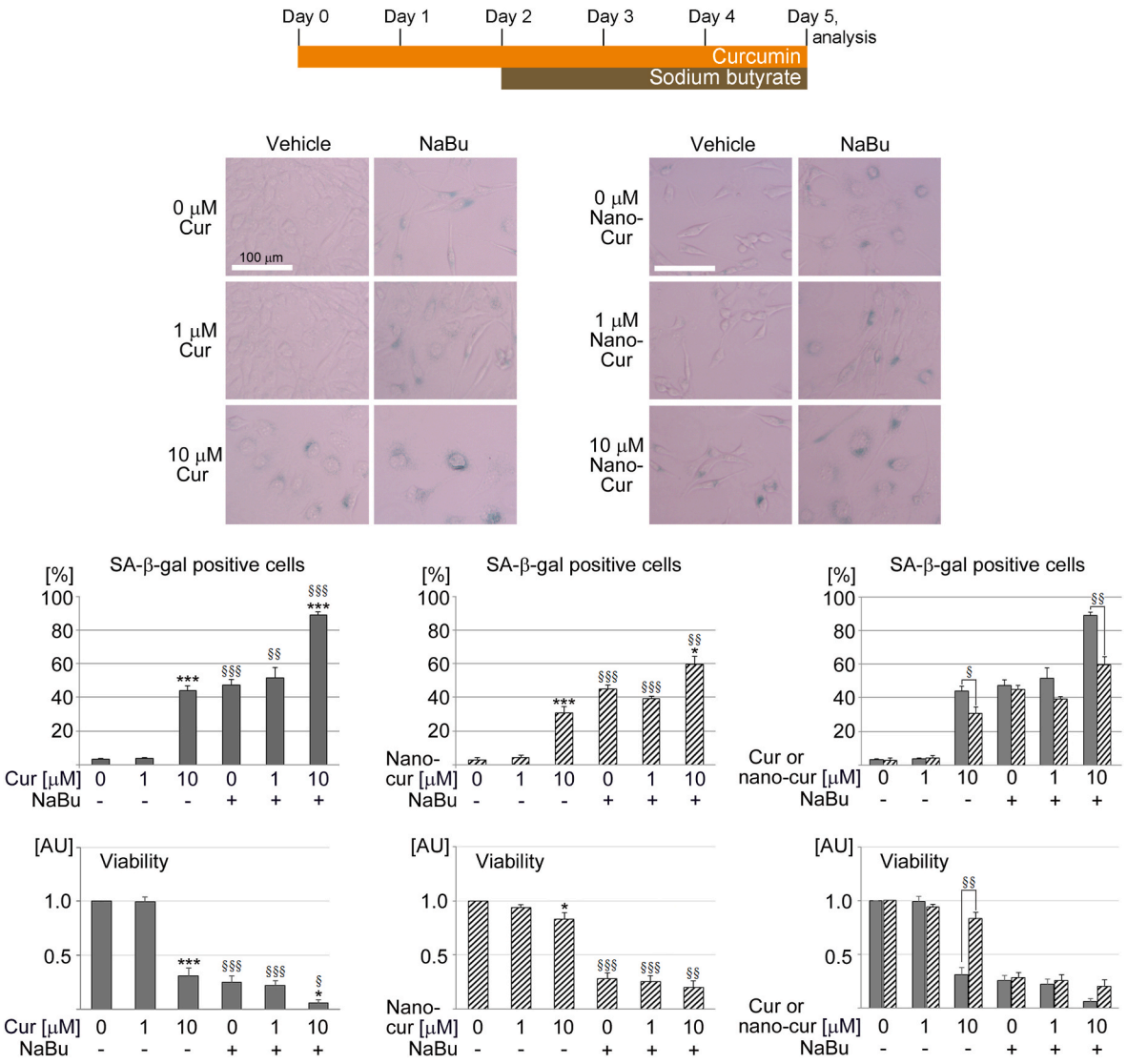

Fig. 3. Free curcumin and nano-curcumin induce cellular senescence in fibroblasts. Experimental design: NIH3T3 cells were pre-incubated with vehicle, free curcumin or nano-curcumin for 2 days. The incubation was continued for three additional days in the absence or presence of sodium butyrate. To monitor cellular senescence, SA-β galactosidase (SA-β-gal) activity was detected with chromogenic assays. Graphs show averages + SEM for three independent experiments (n = 3). At least 100 cells were scored for each data point and every experiment. The viability of fibroblasts was assessed in parallel (bottom). The changes in fibroblast senescence or viability were compared for free curcumin (gray bars) and nano-curcumin (striped bars). Statistical evaluation was conducted with One-way ANOVA and Bonferroni correction. Pairwise comparisons were performed between controls and individual experimental conditions; *, $p < 0.05$; ***, $p < 0.001$. Student's t-test identified significant differences between experimental groups treated without and with sodium butyrate; §, $p < 0.05$; §§, $p < 0.01$; §§§, $p < 0.001$. Student's t-test was applied to compare the results for free curcumin and nano-curcumin (graphs with both gray and striped bars); §, $p < 0.05$; §§, $p < 0.01$. Size bars are 100 µm. NaBu, sodium butyrate; AU, arbitrary units.

lower for free curcumin (Fig. 3). The same trends were observed for curcumin/butyrate combinations. These results confirm that nano-curcumin elicits a milder impact on cell physiology than the free compound (Figs. 2 and 3).

3.3. *Multiple biomarkers confirm that curcumin induces senescence in fibroblasts*

Additional biomarkers independently verified that curcumin promotes fibroblast senescence. Cellular senescence is often accompanied by changes in the abundance of cell cycle regulators, which contribute to cell cycle arrest (Sikora et al., 2021). Curcumin diminished the levels of p21, which were further reduced by butyrate (Fig. 4). As observed previously (Chu et al., 2022), butyrate also decreased p53 levels, but curcumin or nano-curcumin alone had no significant effects. It should be noted that the loss of p21 and p53 is consistent with an established cell cycle arrest (Tripathi et al., 2021). While p21 and p53 commonly limit cell proliferation, a more intricate relationship has emerged for cellular senescence. Thus, the abundance of p21 and p53 diminishes upon induction of senescence when cells have lost their ability to proliferate (Tripathi et al., 2021).

Furthermore, curcumin reduced lamin B abundance (Fig. 4); the loss of lamin B also represents a hallmark of cellular senescence (Sikora et al., 2021). Notably, DNA damage, monitored with the marker γH2AX, did not significantly increase upon incubation with curcumin, nano-curcumin, alone or in combination with butyrate. Taken together, several independent lines of evidence support the hypothesis that curcumin and curcumin/butyrate combinations trigger senescence in fibroblasts. While nano-curcumin elicits the same effects, the outcome was generally less profound when compared to the free compound.

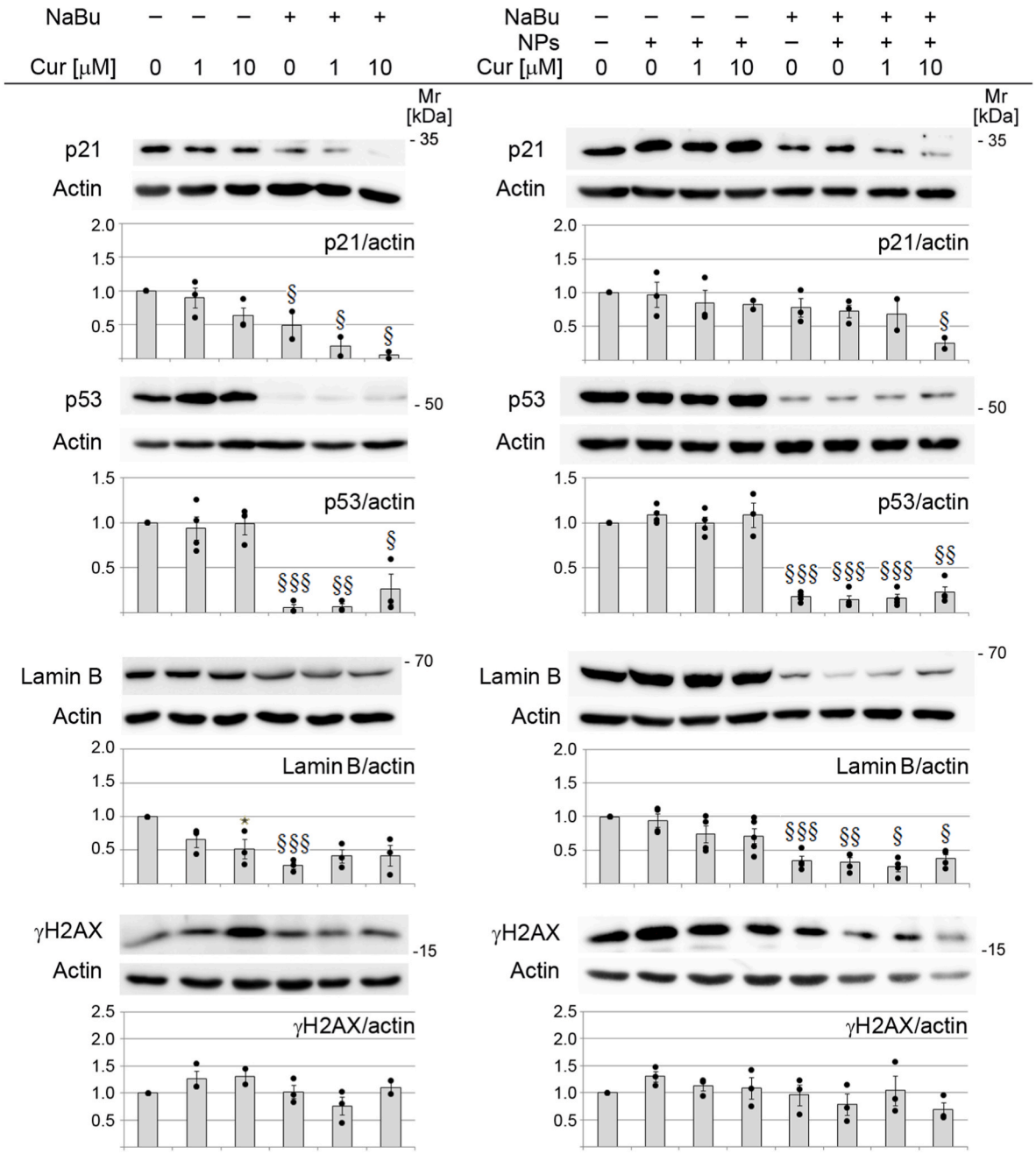

Fig. 4. Evaluation of senescence biomarkers in fibroblasts incubated with curcumin, butyrate, or curcumin/butyrate combinations. NIH3T3 cells were treated with different compounds as described in Materials and methods. Crude cell extracts were used for Western blotting. Results were normalized to vehicle controls. Molecular masses of marker proteins (Mr) in kDa are shown at the right margins of the blots. Graphs depict averages ±SEM for at least two independent experiments (n ≥ 2). Individual data points are represented by black circles, ●. One-way ANOVA with Bonferroni correction revealed significant differences relative to the vehicle control. Comparisons were performed within each experimental group (curcumin alone; curcumin/butyrate combinations); *, $p < 0.05$. Student's t-test identified significant differences that were caused by the addition of butyrate; §, $p < 0.05$; §§, $p < 0.01$; §§§, $p < 0.001$.

3.4. Curcumin, nano-curcumin, and butyrate modulate multiple biomarkers of stress and inflammation

Cellular senescence and organismal aging are associated with increased oxidative stress (George et al., 2022; Liu et al., 2023; Shin et al., 2023) and a rise in inflammation, known as inflammaging (Franceschi et al., 2018). We examined two major regulators of cellular stress responses and inflammation, the transcription factors nuclear factor erythroid 2-related factor 2 (Nrf2, (George et al., 2022)) and nuclear factor kappa-B (NFκB, (Liu et al., 2023)). While butyrate diminished the levels of the transcription factor Nrf2, no obvious trend was observed with curcumin or nano-curcumin (Fig. 5a). For several conditions, Nrf2 migrated as a doublet on denaturing polyacrylamide gels. The ECL signals for both bands were included in the quantification. Different posttranslational modifications have been reported for Nrf2 (Hornbeck et al., 2015), which can explain the observed doublet. The physiological relevance of the doublet will have to be explored in future experiments.

The activation of the transcription factor NFκB is a common consequence of inflammaging. In our model system, the combination of free curcumin and butyrate increased the abundance of NFκB (Fig. 5a). By contrast, nano-curcumin diminished NFκB levels when butyrate was

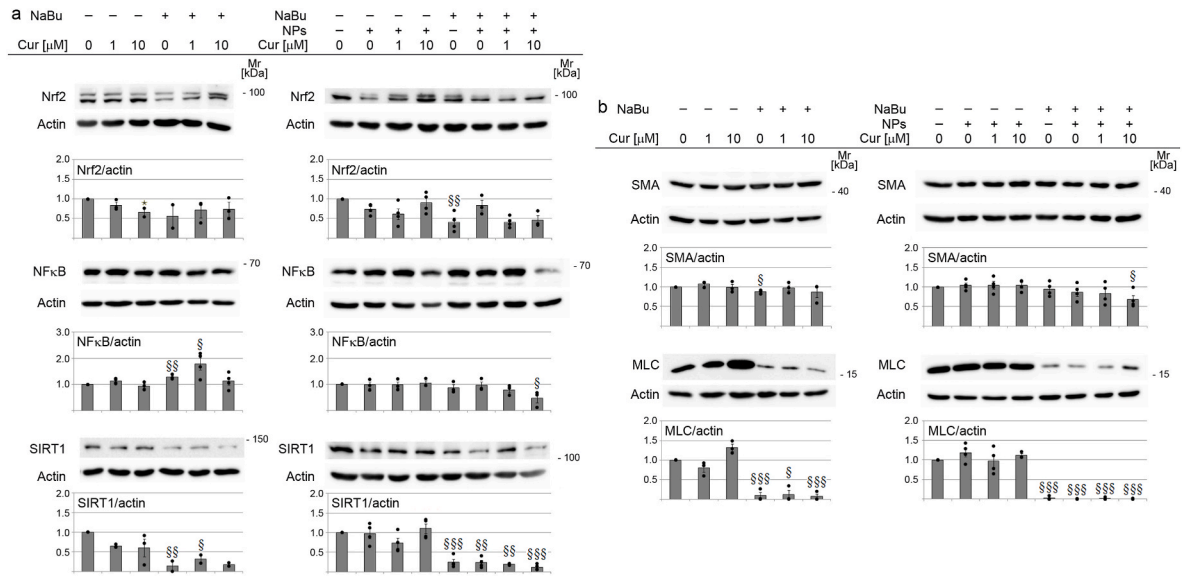

Fig. 5. Evaluation of the fibroblast responses to curcumin, butyrate, and curcumin/butyrate combinations. (a) The abundance of Nrf2, NFκB, and SIRT1, markers of stress and inflammation, was evaluated. (Note that the same blot was used to detect Nrf2 and p21 (Fig. 4). Therefore, the actin panels are identical for Nrf2 and p21.) (b) Markers of fibrosis were examined; SMA, α-smooth muscle actin; MLC, myosin light chain. (a, b) Molecular masses of marker proteins (Mr) in kDa are shown at the right margins of the blots. Results for Western blotting were normalized to vehicle controls. Graphs depict averages ±SEM for at least two independent experiments (n ≥ 2). Individual data points are represented by black circles, ●. One-way ANOVA with Bonferroni correction revealed significant differences relative to the vehicle control. Comparisons were conducted within each experimental group (curcumin alone; curcumin/butyrate combinations); *, $p < 0.05$. Student's t-test identified significant differences due to the addition of butyrate; §, $p < 0.05$; §§, $p < 0.01$; §§§, $p < 0.001$.

present. Thus, under the conditions analyzed, nano-curcumin dampened pro-inflammatory responses more efficiently than free curcumin (Fig. S3).

Profound changes were detected for the lysine deacetylase SIRT1, which is closely linked to aging and aging-associated diseases (He, 2016; You and Liang, 2023). Free curcumin led to a moderate loss in SIRT1 abundance, whereas butyrate caused a marked and significant reduction of SIRT1 levels (Fig. 5a).

3.5. *Butyrate reduces the abundance of myosin light chain, a biomarker of fibrosis*

Wound healing is a complex process that proceeds through several phases; the orderly progression through these phases requires a delicate balance among fibroblast populations with different characteristics. Several aspects of fibroblast biology are relevant to wound healing and our study. First, the transient generation of senescent fibroblasts is a prerequisite for efficient wound healing (Wilkinson and Hardman, 2020). Second, the transition of fibroblasts to myofibroblasts is necessary for wound closure. Third, fibroblast senescence diminishes the fibroblast to myofibroblast transition (López-Antona et al., 2022). Fourth, persistent fibroblast activation is deleterious, as it promotes tissue and organ fibrosis (Migneault and Hébert, 2021; Salminen, 2023). Myofibroblasts are characterized by the elevated production of α-smooth muscle actin (SMA) and myosin light chain (MLC). Curcumin, nano-curcumin, and butyrate did not cause profound changes in SMA abundance (Fig. 5b). As well, curcumin and nano-curcumin had no significant effect on MLC. Notably, MLC was significantly reduced with butyrate (Fig. 5b). This confirms the role of butyrate as a safeguard against the transition of fibroblasts to myofibroblasts.

Curcumin promotes wound healing through its impact on multiple cell types (Akbik et al., 2014). Based on our results, we propose that fibroblast senescence contributes to the curcumin-dependent benefits for tissue repair. The combination of curcumin and butyrate goes beyond the advantages afforded by curcumin alone. We hypothesize that the curcumin/butyrate combination limits fibrosis associated with wound healing through at least two scenarios which are not mutually exclusive. In particular, curcumin/butyrate reduces or limits the growth and transformation of fibroblast at the end of wound healing and/or restricts the progression of fibrosis.

4. Conclusions

Taken together, our study supports the model that free curcumin and nano-curcumin drive fibroblasts into senescence (Fig. 6); this process is further stimulated with butyrate. However, butyrate also significantly reduces the myofibroblast phenotype (Fig. 5b). We propose a possible mechanism that connects these events and is based on the changes of SIRT1 abundance (Fig. 5a). Our focus is on SIRT1, because curcumin stimulates the enzymatic activity of SIRT1, but also its degradation by the proteasome (Zendedel et al., 2018). The curcumin-mediated loss of SIRT1, especially in combination with butyrate, correlates with enhanced fibroblast senescence. The acquisition of a senescent phenotype limits the transition of fibroblasts to myofibroblasts (López-Antona et al., 2022; Salminen, 2023). As a result, hallmarks of tissue fibrosis are reduced.

Compared with free curcumin, nano-curcumin produces qualitatively the same, although milder, reactions. One noteworthy exception is the curtailing of the inflammatory response, indicated by the loss of NFκB for the nano-curcumin/butyrate combination (Fig. 5a). A possible explanation for this phenomenon is a gradual and prolonged exposure of cells to curcumin that is delivered as a nanoformulation. Future experiments will address this question. Taken together, our study sets the stage to develop therapeutic strategies that take advantage of curcumin, either alone or in combination with butyrate, for the therapeutic control of fibroblast senescence.

Ethics approval

Not applicable.

Funding

This work was supported by funds from NSERC (Natural Sciences

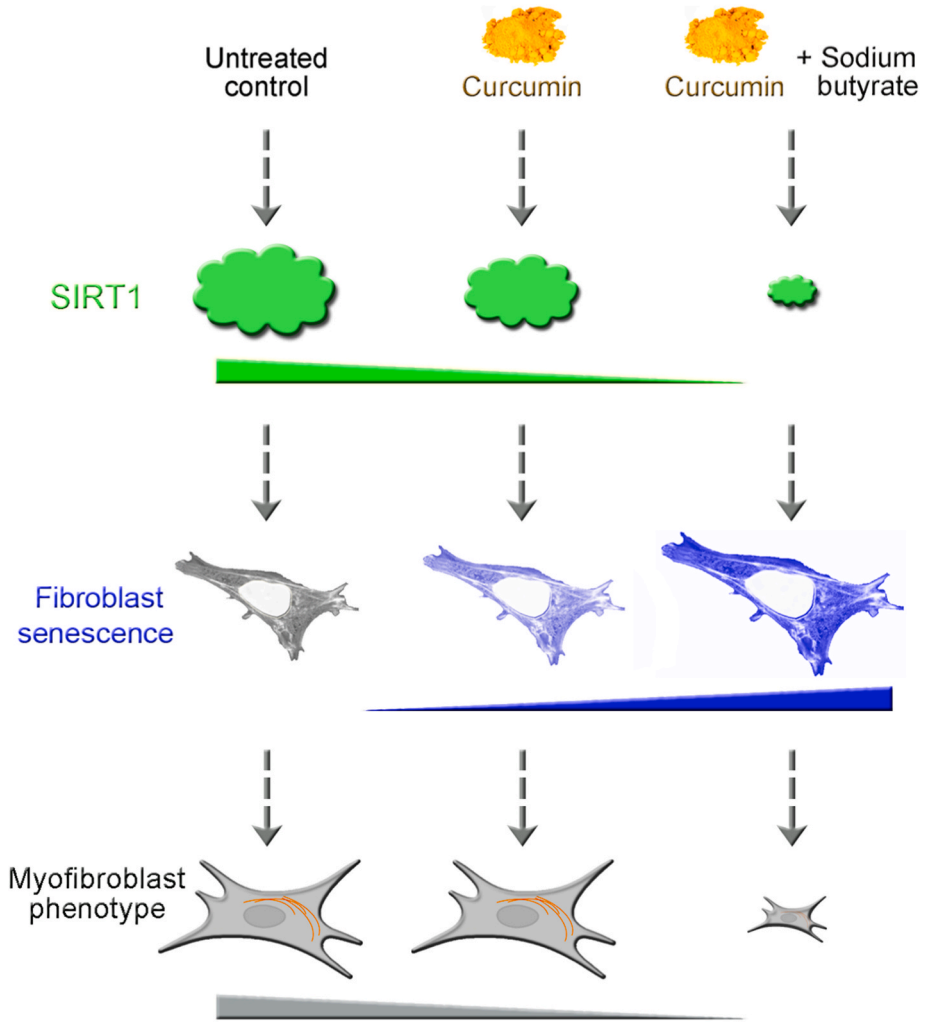

Fig. 6. Model summarizing the effects of curcumin, and curcumin/butyrate combinations on SIRT1 abundance, cellular senescence, and fibrosis. A simplified model links curcumin to fibroblast physiology. We propose that the loss of SIRT1 is a key factor that promotes cellular senescence. This reduces the myofibroblast phenotype in the fibroblast cell population. See text for details.

and Engineering Research Council of Canada) and FRQNT (Fonds de Recherche du Québec Nature et technologies). SC and HWY were supported by fellowships from Fonds de Recherche du Québec - Santé and FRQNT.

Author contributions

Conception and design: S. Chu, U. Stochaj, A. Kakkar, D. Maysinger; Development of methodology: S. Chu, A. Kakkar, H. W. Yong, U. Stochaj; Data acquisition: S. Chu, H. W. Yong, N. Joma, U. Stochaj; Writing and review of manuscript: S. Chu, U. Stochaj, A. Kakkar, D. Maysinger; Funding Acquisition: U. Stochaj, A. Kakkar.

Patient consent

Not applicable.

Permission to reproduce material from other sources

Not applicable.

Data availability

The datasets generated and/or analyzed during this study are available from the corresponding author on reasonable request.

Declaration of competing interest

The authors declare no conflict of interest.

Acknowledgements

We are grateful to Dr. V. Blank (McGill University) for kindly providing us with NIH3T3 cells.

Appendix A. Supplementary data

Supplementary data to this article can be found online at https://doi.org/10.1016/j.amolm.2023.100021.

References

Akbik, D., Ghadiri, M., Chrzanowski, W., et al., 2014. Curcumin as a wound healing agent. Life Sci. 116 (1), 1–7.
Ataei, M., Gumpricht, E., Kesharwani, P., et al., 2023. Recent advances in curcumin-based nanoformulations in diabetes. J. Drug Target. 31 (7), 671–684.
Baghbanbashi, M., Yong, H.W., Zhang, I., et al., 2022. Stimuli-responsive miktoarm polymer-based formulations for fisetin delivery and regulatory effects in hyperactive human microglia. Macromol. Biosci. 22 (10), e2200174.

Bielak-Zmijewska, A., Grabowska, W., Ciolko, A., et al., 2019. The role of curcumin in the modulation of ageing. Int. J. Mol. Sci. 20 (5), 1239.
Chaib, S., Tchkonia, T., Kirkland, J.L., 2022. Cellular senescence and senolytics: the path to the clinic. Nat. Med. 28 (8), 1556–1568.
Chang, W., Wang, Y., Luxton, G.W.G., et al., 2019. Imbalanced nucleocytoskeletal connections create common polarity defects in progeria and physiological aging. Proc. Natl. Acad. Sci. U.S.A. 116 (9), 3578–3583.
Cheng, A.L., Hsu, C.H., Lin, J.K., et al., 2001. Phase I clinical trial of curcumin, a chemopreventive agent, in patients with high-risk or pre-malignant lesions. Anticancer Res. 21 (4b), 2895–2900.
Chriett, S., Dąbek, A., Wojtala, M., et al., 2019. Prominent action of butyrate over β-hydroxybutyrate as histone deacetylase inhibitor, transcriptional modulator and anti-inflammatory molecule. Sci. Rep. 9 (1), 742.
Chu, S., Moujaber, O., Lemay, S., et al., 2022. Multiple pathways promote microtubule stabilization in senescent intestinal epithelial cells. npj Aging 8 (1), 16.
Corrêa, R.O., Castro, P.R., Moser, R., et al., 2022. Butyrate: connecting the gut-lung axis to the management of pulmonary disorders. Front. Nutr. 9, 1011732.
Debacq-Chainiaux, F., Erusalimsky, J.D., Campisi, J., et al., 2009. Protocols to detect senescence-associated beta-galactosidase (SA-betagal) activity, a biomarker of senescent cells in culture and in vivo. Nat. Protoc. 4 (12), 1798–1806.
Dei Cas, M., Ghidoni, R., 2019. Dietary curcumin: correlation between bioavailability and health potential. Nutrients 11 (9), 2147.
El-Saadony, M.T., Yang, T., Korma, S.A., et al., 2022. Impacts of turmeric and its principal bioactive curcumin on human health: pharmaceutical, medicinal, and food applications: a comprehensive review. Front. Nutr. 9, 1040259.
Franceschi, C., Garagnani, P., Parini, P., et al., 2018. Inflammaging: a new immune–metabolic viewpoint for age-related diseases. Nat. Rev. Endocrinol. 14 (10), 576–590.
George, M., Tharakan, M., Culberson, J., et al., 2022. Role of Nrf2 in Aging, Alzheimer's and Other Neurodegenerative Diseases. Ageing Res Rev, 101756.
Han, S., Lu, Q., Liu, X., 2023. Advances in cellular senescence in idiopathic pulmonary fibrosis. Exp. Ther. Med. 25 (4), 145.
He, Y.-Y., 2016. Sirtuins and stress response in skin cancer, aging, and barrier function. In: Wondrak, G.T. (Ed.), Skin Stress Response Pathways: Environmental Factors and Molecular Opportunities. Springer International Publishing, Cham, pp. 251–263.
Heidari, H., Bagherniya, M., Majeed, M., et al., 2023. Curcumin-piperine co-supplementation and human health: a comprehensive review of preclinical and clinical studies. Phytother Res. 37 (4), 1462–1487.
Hornbeck, P.V., Zhang, B., Murray, B., et al., 2015. PhosphoSitePlus, 2014: mutations, PTMs and recalibrations. Nucleic Acids Res. 43 (D1), D512–D520.
Kakkar, A., Traverso, G., Farokhzad, O.C., et al., 2017. Evolution of macromolecular complexity in drug delivery systems. Nat. Rev. Chem 1 (8), 0063.
Kirk, T., Ahmed, A., Rognoni, E., 2021. Fibroblast memory in development, homeostasis and disease. Cells 10 (11), 2840.
Lagoumtzi, S.M., Chondrogianni, N., 2021. Senolytics and Senomorphics: natural and synthetic therapeutics in the treatment of aging and chronic diseases. Free Radic. Biol. Med. 171, 169–190.
Li, L., Zhang, X., Pi, C., et al., 2020. Review of curcumin physicochemical targeting delivery system. Int. J. Nanomed. 15, 9799–9821.
Li, W., Qin, L., Feng, R., et al., 2019. Emerging senolytic agents derived from natural products. Mech. Ageing Dev. 181, 1–6.
Li, Y., Adeniji, N.T., Fan, W., et al., 2022. Non-alcoholic fatty liver disease and liver fibrosis during aging. Aging Dis 13 (4), 1239–1251.
Liu, H.M., Cheng, M.Y., Xun, M.H., et al., 2023. Possible mechanisms of oxidative stress-induced skin cellular senescence, inflammation, and cancer and the therapeutic potential of plant polyphenols. Int. J. Mol. Sci. 24 (4), 3755.
López-Antona, I., Contreras-Jurado, C., Luque-Martín, L., et al., 2022. Dynamic regulation of myofibroblast phenotype in cellular senescence. Aging Cell 21 (4), e13580.
Lotocki, V., Kakkar, A., 2020. Miktoarm star polymers: branched architectures in drug delivery. Pharmaceutics 12 (9), 827.
Lotocki, V., Yazdani, H., Zhang, Q., et al., 2021. Miktoarm star polymers with environment-selective ROS/GSH responsive locations: from modular synthesis to tuned drug release through micellar partial corona shedding and/or core. Disassembly. Macromol. Biosci. 21 (2), e2000305.
Mahjoob, M., Stochaj, U., 2021. Curcumin nanoformulations to combat aging-related diseases. Ageing Res. Rev. 69, 101364.
McElhinney, K., Irnaten, M., O'Brien, C., 2023. p53 and myofibroblast apoptosis in organ fibrosis. Int. J. Mol. Sci. 24 (7), 6737.
Migneault, F., Hébert, M.J., 2021. Autophagy, tissue repair, and fibrosis: a delicate balance. Matrix Biol. 100–101, 182–196.
Moquin, A., Sturn, J., Zhang, I., et al., 2019. Unraveling aqueous self-assembly of telodendrimers to shed light on their efficacy in drug encapsulation. ACS Appl. Bio Mater. 2 (10), 4515–4526.
Moujaber, O., Fishbein, F., Omran, N., et al., 2019. Cellular senescence is associated with reorganization of the microtubule cytoskeleton. Cell. Mol. Life Sci. 76 (6), 1169–1183.
NIH, Clinical Trials; National Institute of Health. Clinical trials on senolytics. https://clinicaltrials.gov/search?term=senolytic.
Park, H.J., Jeong, O.Y., Chun, S.H., et al., 2021. Butyrate improves skin/lung fibrosis and intestinal dysbiosis in bleomycin-induced mouse models. Int. J. Mol. Sci. 22 (5), 2765.
Plikus, M.V., Wang, X., Sinha, S., et al., 2021. Fibroblasts: origins, definitions, and functions in health and disease. Cell 184 (15), 3852–3872.
Ring, N.A.R., Valdivieso, K., Grillari, J., et al., 2022. The role of senescence in cellular plasticity: lessons from regeneration and development and implications for age-related diseases. Dev. Cell 57 (9), 1083–1101.
Riss, T.L., Moravec, R.A., Niles, A.L., et al., 2013. Cell viability assays [updated 2016]. In: Markossian, Sarine, et al. (Eds.), Assay Guidance Manual. Eli Lilly & Company and the National Center for Advancing Translational Sciences; 2004-. Bethesda (MD).
Robbins, P.D., Jurk, D., Khosla, S., et al., 2020. Senolytic drugs: reducing senescent cell viability to extend health span. Annu. Rev. Pharmacol. Toxicol. 61, 779–803.
Salminen, A., 2023. The Plasticity of Fibroblasts: A Forgotten Player in the Aging Process. Ageing Res Rev, 101995.
Shin, S.H., Lee, Y.H., Rho, N.K., et al., 2023. Skin aging from mechanisms to interventions: focusing on dermal aging. Front. Physiol. 14, 1195272.
Sikora, E., Bielak-Zmijewska, A., Mosieniak, G., 2021. A common signature of cellular senescence; does it exist? Ageing Res. Rev. 71, 101458.
Soliman, G.M., Sharma, R., Choi, A.O., et al., 2010. Tailoring the efficacy of nimodipine drug delivery using nanocarriers based on A2B miktoarm star polymers. Biomaterials 31 (32), 8382–8392.
Todaro, G.J., Green, H., 1963. Quantitative studies of the growth of mouse embryo cells in culture and their development into established lines. J. Cell Biol. 17 (2), 299–313.
Tripathi, U., Misra, A., Tchkonia, T., et al., 2021. Impact of senescent cell subtypes on tissue dysfunction and repair: importance and research questions. Mech. Ageing Dev. 198, 111548.
Uzarski, J.S., DiVito, M.D., Wertheim, J.A., et al., 2017. Essential design considerations for the resazurin reduction assay to noninvasively quantify cell expansion within perfused extracellular matrix scaffolds. Biomaterials 129, 163–175.
Wilkinson, H.N., Hardman, M.J., 2020. Senescence in wound repair: emerging strategies to target chronic healing wounds. Front. Cell Dev. Biol. 8, 773.
Yi, C., Liu, J., Deng, W., et al., 2023. Old age promotes retinal fibrosis in choroidal neovascularization through circulating fibrocytes and profibrotic macrophages. J. Neuroinflammation 20 (1), 45.
Yong, H.W., Kakkar, A., 2021. Nanoengineering branched star polymer-based formulations: scope, strategies, and advances. Macromol. Biosci. 21 (8), e2100105.
You, Y., Liang, W., 2023. SIRT1 and SIRT6: the role in aging-related diseases. Biochim. Biophys. Acta, Mol. Basis Dis., 166815
Zendedel, E., Butler, A.E., Atkin, S.L., et al., 2018. Impact of curcumin on sirtuins: a review. J. Cell. Biochem. 119 (12), 10291–10300.